Department of Electrical Engineering

Dynamic induction machine models including magnetic saturation and iron losses

Mikaela Ranta

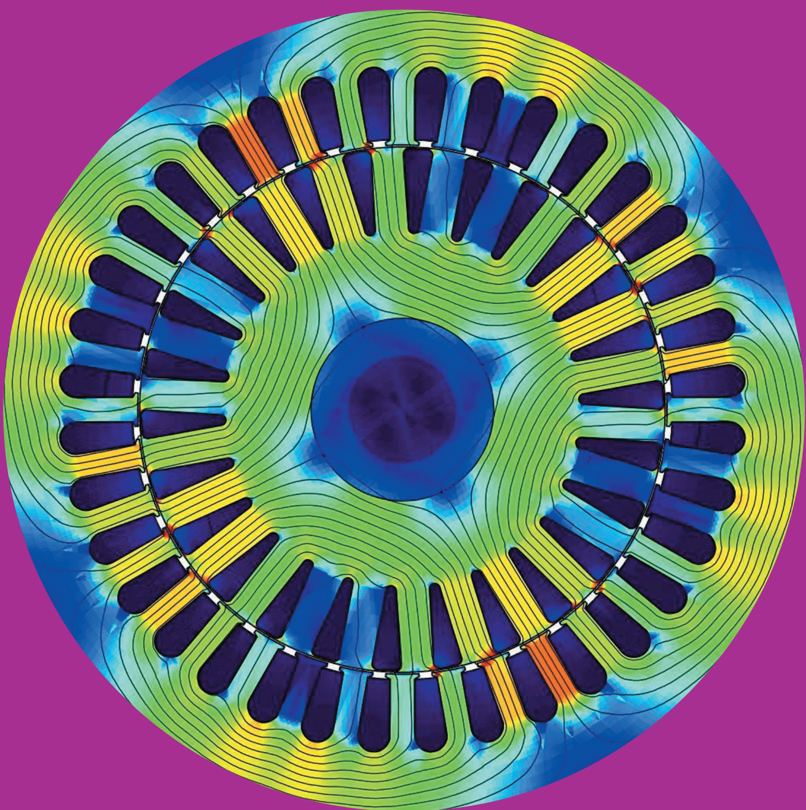

DOCTORAL DISSERTATIONS

Aalto University publication series
DOCTORAL DISSERTATIONS 171/2013

Dynamic induction machine models including magnetic saturation and iron losses

Mikaela Ranta

A doctoral dissertation completed for the degree of Doctor of Science (Technology) to be defended, with the permission of the Aalto University School of Electrical Engineering, at a public examination held at the lecture hall S5 of the school on 29 November 2013 at 12.

Aalto University
School of Electrical Engineering
Department of Electrical Engineering
Electric drives

Supervising professors
Prof. Jorma Luomi
Prof. Marko Hinkkanen

Thesis advisor
Prof. Marko Hinkkanen

Preliminary examiners
Prof. Jan Melkebeek, Ghent University, Belgium
Prof. Joaquín Pedra, Universitat Politècnica de Catalunya, Spain

Opponent
Prof. Torbjörn Thiringer, Chalmers University of Technology, Sweden

Aalto University publication series
DOCTORAL DISSERTATIONS 171/2013

© Mikaela Ranta

ISBN 978-952-60-5395-0
ISBN 978-952-60-5396-7 (pdf)
ISSN-L 1799-4934
ISSN 1799-4934 (printed)
ISSN 1799-4942 (pdf)
http://urn.fi/URN:ISBN:978-952-60-5396-7

Unigrafia Oy
Helsinki 2013

Finland

441 697
Printed matter

Aalto University

Aalto University, P.O. Box 11000, FI-00076 Aalto www.aalto.fi

Abstract

Author
Mikaela Ranta

Name of the doctoral dissertation
Dynamic induction machine models including magnetic saturation and iron losses

Publisher School of Electrical Engineering

Unit Department of Electrical Engineering

Series Aalto University publication series DOCTORAL DISSERTATIONS 171/2013

Field of research Electric drives

Manuscript submitted 21 May 2013 **Date of the defence** 29 November 2013

Permission to publish granted (date) 8 August 2013 **Language** English

☐ **Monograph** ☒ **Article dissertation (summary + original articles)**

Abstract

Dynamic induction machine models are used as the basis for the design and implementation of control algorithms. Costs can be reduced by applying speed-sensorless control, and advanced control strategies open up for the possibility of using an induction machine in demanding applications. However, a reliable and good control performance requires more detailed induction machine models. This thesis deals with models including the magnetic saturation and iron losses. A small-signal model, which includes the saturation due to variations in the main flux magnitude and the load torque, is used to analyze the transient behavior of the machine. Due to the magnetic saturation, the inductances vary as a function of the operating point, and the machine appears to be salient in transients. Based on the model, an identification method for the leakage inductance is proposed. The identification is based on signal injection and can be performed as the machine is running under different load conditions. A model for the skin effect of the rotor bars can be used in combination with the leakage inductance identification in the case of an induction machine equipped with deep rotor bars. The magnetizing curve can be modeled using a simple power function. An adaptive identification method is developed for the identification of magnetizing curve parameters. Identification of the leakage inductance prior to the magnetizing curve identification improves the results in case a no-load condition cannot be reached. The stator hysteresis and eddy current losses are modeled using a nonlinear resistance. The resistance is not dependent on any frequency, and is thus defined also during transients. The resistance model is experimentally investigated both for the case of an induction machine and a nonlinear inductor. The iron loss model is used in a loss-minimizing control algorithm for the induction machine.

Keywords induction machines, dynamic models, magnetic saturation, iron losses

ISBN (printed) 978-952-60-5395-0 **ISBN (pdf)** 978-952-60-5396-7

ISSN-L 1799-4934 **ISSN (printed)** 1799-4934 **ISSN (pdf)** 1799-4942

Location of publisher Helsinki **Location of printing** Helsinki **Year** 2013

Pages 138 **urn** http://urn.fi/URN:ISBN:978-952-60-5396-7

A! Aalto-universitetet

Aalto-universitetet, PB 11000, 00076 Aalto www.aalto.fi

Sammandrag

Författare
Mikaela Ranta

Doktorsavhandlingens titel
Dynamiska modeller av induktionsmotorn inklusive magnetisk mättnad och kärnförluster

Utgivare Högskolan för elektroteknik

Enhet Institutionen för elektroteknik

Seriens namn Aalto University publication series DOCTORAL DISSERTATIONS 171/2013

Forskningsområde Elektriska drivsystem

Inlämningsdatum för manuskript 21.05.2013 **Datum för disputation** 29.11.2013

Beviljande av publiceringstillstånd (datum) 08.08.2013 **Språk** Engelska

☐ **Monografi** ☒ **Sammanläggningsavhandling (sammandrag plus separata artiklar)**

Sammandrag

Dynamiska modeller av induktionsmotorn används som grund för att utforma och tillämpa styralgoritmer. Kostnadseffektiva lösningar kan uppnås genom att tillämpa styrsystem utan varvtalsmätare, dessutom har avancerade styrsystem möjliggjort att induktionsmotorn även används i mer krävande användningsområden. För att åstadkomma bra prestanda behövs emellertid mer detaljerade modeller av induktionsmotorn. Denna avhandling handlar om modeller som inkluderar magnetisk mättnad och kärnförluster. Maskinens transienta egenskaper analyseras med hjälp av en småsignalmodell som inkluderar magnetisk mättnad orsakad av variationer i det magnetiska flödet och vridmomentet. Induktanserna i modellen varierar som funktion av arbetspunkten p.g.a. den magnetiska mättnaden, och maskinen förefaller ha utpräglade poler vid transienta förlopp. En identifieringsmetod för läckinduktansen föreslås på basen av modellen. Identifieringsmetoden baseras på injicerade signaler och kan utföras under normal användning av maskinen och vid olika grad av belastning. En modell för skineffekten i rotorn kan användas i kombination med identifieringsmetoden för maskiner som har djupa rotorspår. Magnetiseringskurvan kan beskrivas med en enkel potensfunktion. En adaptiv identifieringsmetod utvecklas för att identifiera magnetiseringskurvans parametrar. Om identifieringen inte kan utföras utan belastning, förbättras resultatet genom att identifiera läckinduktansen före magnetiseringskurvan. Hysteres- och virvelströmsförluster i statorn modelleras genom att använda en icke-linjär resistans. Frekvensen ingår ej som parameter i resistansfunktionen och resistansen är därmed definerbar också i transienta förlopp. Modellen för kärnförluster undersöks experimentellt både för en induktionsmotor och en icke-linjär induktor. Modellen implementeras även i en algoritm för minimering av förlusterna i en induktionsmotor.

Nyckelord induktionsmotor, dynamiska modeller, magnetisk mättnad, kärnförluster

ISBN (tryckt) 978-952-60-5395-0 **ISBN (pdf)** 978-952-60-5396-7

ISSN-L 1799-4934 **ISSN (tryckt)** 1799-4934 **ISSN (pdf)** 1799-4942

Utgivningsort Helsingfors **Tryckort** Helsingfors **År** 2013

Sidantal 138 **urn** http://urn.fi/URN:ISBN:978-952-60-5396-7

Preface

I started the research for this thesis in 2006 as part of a project aimed at developing methods for sensorless control of electrical machines. The work has been carried out in the Electrical department at the School of Electrical Engineering, and has been financed by ABB Oy. I also greatly acknowledge the financial support from Emil Aaltosen Säätiö and the Research Foundation of Helsinki University of Technology.

First of all I am very grateful to Prof. Jorma Luomi who offered me the position as a Ph.D. student. His insightful comments on the topic and scientific writing have been of great value. I am sad he is no longer here to see the work being finished. Throughout the work, I have got guidance from Prof. Marko Hinkkanen, and the last year he also acted as my supervisor. I want to thank him for all his helpful comments and ideas, without them I do not thing I could have done this work. I also want to thank Prof. Antero Arkkio who shared his expertise on electrical machines.

The cooperation and discussions with Dr. Anna-Kaisa Repo have been of much help, because of her I never had to deal with the finite element analysis myself. I am also happy that I have been able to use the results of Mr. Toni Tuovinen's work on magnetic saturation of induction machines. I greatly appreciate the discussions and cooperation with Prof. Anouar Belahcen, Dr. Emad Dlala and Mr. Zengcai Qu, who shared their expertise on iron losses and motor control.

I am grateful to my colleagues Dr. Janne Salomäki, Dr. Antti Piippo, Mr. Toni Tuovinen, Mr. Seppo Saarakkala, Mr. Jarno Kukkola, Mr Zengcai Qu, Mr. Matti Liukkonen, Mr. Taneli Tiainen, and Mr. Jussi Koppinen who have created a relaxed and friendly working atmosphere. I also want to thank the rest of the staff at the Electrical department. Whenever I have had a problem of some kind, there has been someone able to offer help.

Having children is perhaps not the best way to gain success in the academic world, but they have helped me in their own ways. My son Toivo's happy mood has given me a lot of energy, and I might never have finished if my daughter Lykke would not have set a deadline I just could not miss. Finally, I would like to thank my husband Mika for all love and support in my good times as well as in my bad times.

Espoo, October 16, 2013,

Mikaela Ranta

Contents

List of Publications

This thesis consists of an overview and of the following publications which are referred to in the text by their Roman numerals.

I M. Ranta, M. Hinkkanen, A.-K. Repo, and J. Luomi. Small-signal analysis of a saturated induction motor. In *Nordic Workshop on Power and Industrial Electronics (NORPIE) 2008*, Espoo, Finland, June 2008.

II M. Ranta, M. Hinkkanen, and J. Luomi. Inductance identification of an induction machine taking load-dependent saturation into account. In *International Conference on Electrical Machines (ICEM) 2008*, Vilamoura, Portugal, September 2008.

III M. Ranta, M. Hinkkanen, E. Dlala, A.-K. Repo, and J. Luomi. Inclusion of hysteresis and eddy current losses in dynamic induction machine models. In *IEEE International Electric Machines & Drives Conference (IEMDC) 2009*, Miami, Florida, May 2009.

IV M. Ranta, M. Hinkkanen, and J. Luomi. Rotor parameter identification of saturated induction machines. In *IEEE Energy Conversion Congress and Exposition (ECCE) 2009*, San Jose, California, September 2009.

V M. Hinkkanen, A.-K. Repo, M. Ranta, and J. Luomi. Small-signal modeling of mutual saturation in induction machines. *IEEE Transactions on Industry Applications*, vol. 46, issue 3, pp. 965–973, May-June 2010.

VI M. Ranta, M. Hinkkanen, A. Belahcen, and J. Luomi. Inclusion of hysteresis and eddy current losses in nonlinear time-domain inductance models. In *37th Annual Conference of the IEEE Industrial Electronics Society (IECON) 2011*, Melbourne, Australia, November 2011.

VII Z. Qu, M. Ranta, M. Hinkkanen, and J. Luomi. Loss-minimizing flux level control of induction motor drives. *IEEE Transactions on Industry Applications*, vol. 48, issue 3, pp. 952–961, May-June 2012.

VIII M. Ranta and M. Hinkkanen. Online identification of parameters defining the saturation characteristics of induction machines. *IEEE Transactions on Industry Applications*, vol. 49, issue 5, pp. 2136–2145, Sept.-Oct. 2013.

Author's Contribution

Publication I: "Small-signal analysis of a saturated induction motor"

The author wrote the paper under the guidance of Prof. Luomi and Prof. Hinkkanen. The measurements and the analysis of the results were performed by the author. Dr. Repo performed the finite element analysis.

Publication II: "Inductance identification of an induction machine taking load-dependent saturation into account"

The author wrote the paper under the guidance of Prof. Luomi and Prof. Hinkkanen.

Publication III: "Inclusion of hysteresis and eddy current losses in dynamic induction machine models"

The author wrote the paper in cooperation with Prof. Hinkkanen, Dr. Dlala, and Dr. Repo under the guidance of Prof. Luomi. The author was responsible for the simulation and experimental results.

Publication IV: "Rotor parameter identification of saturated induction machines"

The author wrote the paper under the guidance of Prof. Hinkkanen and Prof. Luomi.

Publication V: "Small-signal modeling of mutual saturation in induction machines"

The author participated in the writing of the paper and performed the measurements and the analysis of the experimental results.

Publication VI: "Inclusion of hysteresis and eddy current losses in nonlinear time-domain inductance models"

The author wrote the paper under the guidance of Prof. Hinkkanen and Prof. Luomi. Prof. Belahcen was responsible for the experimental results.

Publication VII: "Loss-minimizing flux level control of induction motor drives"

The author performed the measurements in cooperation with Mr. Qu. The author also performed the parameter sensitivity analysis and participated in the writing of the paper.

Publication VIII: "Online identification of parameters defining the saturation characteristics of induction machines"

The author wrote the paper under the guidance of Prof. Hinkkanen.

Symbols

c	Saturation function parameter
d	Saturation function parameter
$\mathbf{I}$	Identity matrix
i_a, i_b, i_c	Phase currents
$\boldsymbol{i}_\mathrm{M}$	Magnetizing current of inverse-Γ model
$\boldsymbol{i}_\mathrm{m}$	Magnetizing current
i_m	Magnetizing current magnitude
$\boldsymbol{i}'_\mathrm{M}$	Magnetizing current of Γ model
$\boldsymbol{i}_\mathrm{r}$	Rotor current
i_r	Rotor current magnitude
$\boldsymbol{i}'_\mathrm{R}$	Rotor current of Γ model
$\boldsymbol{i}_\mathrm{s}$	Stator current in synchronous coordinates
i_s0	Operating-point stator current magnitude
$\boldsymbol{i}_\mathrm{s0}$	Operating-point stator current
$\boldsymbol{i}^\mathrm{s}_\mathrm{s}$	Stator current in stator coordinates
$i_{\mathrm{s}\alpha}$, $i_{\mathrm{s}\beta}$	Real and imaginary components of stator current in stator coordinates
$\mathbf{J}$	Orthogonal rotation matrix
k	Iron loss model parameter
L_dd, L_dq, L_qd, L_qq	Leakage inductance matrix elements

L_{M}	Magnetizing inductance of inverse-Γ model
L_{m}	Magnetizing inductance
L_{mdd}, L_{mdq}, L_{mqd}, L_{mqq}	Magnetizing inductance matrix elements
$\boldsymbol{L}_{\mathrm{m}}$	Magnetizing inductance matrix
L_{m0}	Operating-point magnetizing inductance
L_{mt}	Incremental magnetizing inductance
L_{mt0}	Incremental magnetizing inductance
L_{mu}	Unsaturated magnetizing inductance
L_{r}	Rotor inductance
$L_{\mathrm{r}\sigma}$	Rotor leakage inductance
$L_{\mathrm{r}\sigma\mathrm{t}}$	Incremental rotor leakage inductance
L_{s}	Stator inductance
L_{su}	Unsaturated stator inductance
$L_{\mathrm{s}\sigma}$	Stator leakage inductance
L_{σ}	Leakage inductance of inverse-Γ model
$\boldsymbol{L}_{\sigma}$	Leakage inductance matrix
L'_{σ}	Leakage inductance of Γ model
L_{t}	Mutual inductance
n	Iron loss model parameter
R_{Ft}	Eddy current loss resistance
R_{Hy}	Hysteresis loss resistance
R_{r}	Rotor resistance
R_{s}	Stator resistance
$\boldsymbol{R}_{\sigma}$	Total resistance matrix
S	Saturation function parameter
T_{e}	Electromagnetic torque

$\boldsymbol{u}_{\mathrm{s}}$	Stator voltage
u_{s0}	Operating-point stator voltage magnitude
$\boldsymbol{u}_{\mathrm{s0}}$	Operating-point stator voltage
$\boldsymbol{Z}_{\mathrm{s}}$	Impedance matrix
α	Saturation function parameter
β	Saturation function parameter
γ	Saturation function parameter
θ	Angle of reference frame
ϑ_{m0}	Angle of operating-point magnetizing current
$\boldsymbol{\psi}_{\mathrm{m}}$	Main flux linkage
ψ_{m}	Main flux linkage magnitude
$\tilde{\psi}_{\mathrm{md}}$, $\tilde{\psi}_{\mathrm{mq}}$	Deviation in real and imaginary part of main flux
$\boldsymbol{\psi}_{\mathrm{R}}$	Rotor flux linkage of inverse-Γ model
$\boldsymbol{\psi}_{\mathrm{r}}$	Rotor flux linkage
$\boldsymbol{\psi}'_{\mathrm{R}}$	Rotor flux linkage of Γ model
$\boldsymbol{\psi}_{\mathrm{r}\sigma}$	Rotor leakage flux linkage
$\boldsymbol{\psi}_{\mathrm{s}}$	Stator flux linkage
$\boldsymbol{\psi}_{\mathrm{s}\sigma}$	Stator leakage flux linkage
ω_{m}	Electrical angular speed of rotor
ω_{r}	Slip angular frequency
ω_{s}	Stator angular frequency
ω_{s0}	Operating-point stator frequency

1. Introduction

1.1 Background

The induction machine is today the most widely used electrical machine. It is relatively cheap and robust and can be used in various applications. The development of the frequency converter in the 60s and 70s enabled the use of induction machines in variable speed drives. Thus, there is no need to use the less energy efficient and more maintenance demanding DC machine. The development of speed-sensorless control strategies has enabled a considerable reduction in the cost of the drive. Advanced control strategies have also enabled the use of loss-minimizing control that can reduce the amount of energy consumed and, thus, also the operating costs.

The most simple control strategy is the Volts-per-Hertz control (V/f-control), i.e., the stator voltage is controlled to be proportional to the frequency. The stator flux thus remains close to the rated value in all operating points. In applications where the demand for a good dynamic response is high, vector control or direct torque control (DTC) is normally used. Vector control enables decoupling of the magnetic flux and the torque, i.e., the flux and the torque can be controlled independently from each other. Vector control can be applied either as speed-sensored or speed-sensorless. Of these, the speed-sensorless control is more desirable but also more demanding.

A good control performance means, first of all, that the speed or torque is equal to its reference value in steady state. For this to be possible in speed-sensorless applications, the speed needs to be estimated. The decoupling of the magnetic flux and the torque requires the estimation of the position of the flux. The magnitude of the flux is normally kept constant, but, for instance, in loss-minimizing applications, the flux magnitude is also controlled. A good control performance also means that the response to variations in the control input is fast and the overshoot in the controlled signals is minimized. In order to achieve this, the control algorithms should be properly designed and the controllers need to be properly tuned. The estimation of controlled signals and the control algorithms are all based on a model of the machine. Hence, a good performance of the drive requires a model that gives the necessary signals with sufficient accuracy. For the control of the machine, a model describing the fundamental-wave characteristics is normally enough. However, the parameters of the model have to be identified during the self-commissioning of the drive and in some cases also as the machine is running. Some identification techniques are based on transient or higher-frequency signals, and might, therefore, require a more detailed model of the machine.

The induction machine has traditionally been modeled by the so-called T-model. The basic T-model includes five parameters: two resistances and three inductances. In the most simple case, constant-valued parameters are used, that is, the parameter values do not depend on the operating point. However, this kind of model is not optimal for control of the machine. As the machine is loaded, the currents and losses increase and large temperature variations occur. For instance, a temperature rise of 100 °C leads to about a 40% increase in the resistances. A varying flux magnitude, on the other hand, causes variations in the saturation level, and as a result, the inductances vary. Furthermore, iron losses, which are dependent on both the flux magnitude and the frequency, are not at all included in typical dynamic models.

In order to improve the accuracy of the control, more advanced machine models have been proposed. Commonly, the saturation in the main flux path is modelled by adjusting the magnetizing inductance as a function of the magnetizing current. In some models, the saturation of the rotor leakage flux as a function of the rotor current is also included. The iron losses are normally included by adding a resistor in parallel to the stator inductance or magnetizing inductance. An even more detailed model can be achieved by adding iron loss resistors in the rotor branch.

A thermal model could be used to update resistance estimates as the temperature varies. However, a thermal model of the machine would require a lot of data, and as the temperature variations are slow, they can be taken into account by adaptation of the resistances. The rotor time constant is an important parameter in speed-sensored control applications, and the tracking of variations in this parameter due to temperature variations has gained a lot of interest. Adaptation methods for the stator resistance have been developed in order to obtain a robust control performance at low speeds.

The induction machine model still needs refinement. Particularly in machines having skewed or closed rotor slots, the modeling of the magnetic saturation is complicated. The magnetizing inductance is dependent not only on the main flux level, but also on the torque. Similarly, the rotor leakage inductance varies as a function of the flux and torque level. By taking these phenomena into account, the performance of the drive could be improved. Furthermore, the saturation characteristics affect the transient behavior of the machine. The identification of the leakage inductance, for instance, is often based on some transient phenomena. If the effects of the saturation are not taken into account when applying this kind of identification method, large errors might unintentionally occur. Conventional iron loss models, on the other hand, normally consist of a constant-valued resistance and do not properly include the hysteresis losses.

1.2 Objective and Outline of the Thesis

The aim of this thesis is to improve the induction machine model in order to obtain a better control performance. Thus, the focus is on models used in real-time applications for the control of the drive. A small-signal model including the magnetic saturation is used for analysis of the transient behavior of the machine. Based on the model, a method for leakage inductance identification is developed. An adaptive method for the magnetizing curve identification is also proposed. The highest accuracy of the obtained magnetizing curve is achieved if the identification is performed in a no-load condition, but satisfying results can be obtained also under load when the leakage inductance is identified prior to the magnetizing curve.

The iron losses are taken into account by adding a nonlinear resistance to the induction machine model. The resistance is designed to include both the eddy current and hysteresis losses. Further, the skin effect and eddy currents in the rotor bars are modeled by resistances on the rotor side in order to improve the identification results of the leakage inductance when the machine is equipped with deep rotor bars.

The conventional equivalent circuits often used in control applications are shortly presented in Chapter 2. Chapter 3 deals with models including the effects of magnetic saturation and the identification of inductances of a saturated induction machine. Chapter 4 deals with the iron loss models. A summary and the abstract of the publications are given in Chapter 5. Chapter 6 concludes the thesis.

2. Induction Machine Models

2.1 Space Vectors

Normally, the induction machine is delta-connected, or the neutral point of a wye-connection winding is not connected. The zero-sequence component can, therefore, be omitted, and the three-phase winding can be described by two components. As an example, the space vector of the stator current in stator coordinates is obtained based on the stator phase currents from

$$\boldsymbol{i}_{\mathrm{s}}^{\mathrm{s}} = \begin{bmatrix} i_{\mathrm{s}\alpha} \\ i_{\mathrm{s}\beta} \end{bmatrix} = \begin{bmatrix} \frac{2}{3} & -\frac{1}{3} & -\frac{1}{3} \\ 0 & \frac{1}{\sqrt{3}} & -\frac{1}{\sqrt{3}} \end{bmatrix} \begin{bmatrix} i_a \\ i_b \\ i_c \end{bmatrix} \tag{2.1}$$

The stator current can be transformed to any other reference frame according to

$$\boldsymbol{i}_{\mathrm{s}} = \begin{bmatrix} i_{\mathrm{sd}} \\ i_{\mathrm{sq}} \end{bmatrix} = \mathrm{e}^{-\mathbf{J}\theta} \boldsymbol{i}_{\mathrm{s}}^{\mathrm{s}} = [\cos(\theta)\mathbf{I} - \sin(\theta)\mathbf{J}] \boldsymbol{i}_{\mathrm{s}}^{\mathrm{s}} \tag{2.2}$$

where θ is the angle of the reference frame in respect to the stator coordinates. The identity matrix and the orthogonal rotation matrix are

$$\mathbf{I} = \begin{bmatrix} 1 & 0 \\ 0 & 1 \end{bmatrix}, \quad \mathbf{J} = \begin{bmatrix} 0 & -1 \\ 1 & 0 \end{bmatrix} \tag{2.3}$$

respectively.

2.2 Induction Machine Model

In synchronous coordinates rotating at the stator angular frequency ω_{s}, the induction machine can be described by the equations

$$\frac{\mathrm{d}\boldsymbol{\psi}_{\mathrm{s}}}{\mathrm{d}t} = \boldsymbol{u}_{\mathrm{s}} - R_{\mathrm{s}} \boldsymbol{i}_{\mathrm{s}} - \omega_{\mathrm{s}} \mathbf{J} \boldsymbol{\psi}_{\mathrm{s}} \tag{2.4}$$

$$\frac{\mathrm{d}\boldsymbol{\psi}_\mathrm{r}}{\mathrm{d}t} = -R_\mathrm{r}\boldsymbol{i}_\mathrm{r} - \omega_\mathrm{r}\mathbf{J}\boldsymbol{\psi}_\mathrm{r} \tag{2.5}$$

where $\boldsymbol{\psi}_\mathrm{s}$ and $\boldsymbol{\psi}_\mathrm{r}$ are the stator flux linkage and the rotor flux linkage, respectively. The stator voltage is denoted by $\boldsymbol{u}_\mathrm{s}$, the stator current by $\boldsymbol{i}_\mathrm{s}$, and the rotor current by $\boldsymbol{i}_\mathrm{r}$. The stator resistance is R_s and the rotor resistance R_r. The slip angular frequency is $\omega_\mathrm{r} = \omega_\mathrm{s} - \omega_\mathrm{m}$, where ω_m is the electrical rotor speed. The electromagnetic torque can be expressed as

$$T_\mathrm{e} = \boldsymbol{i}_\mathrm{s}^\mathrm{T}\mathbf{J}\boldsymbol{\psi}_\mathrm{s} \tag{2.6}$$

when per-unit values are used.

The relationship between the currents and the flux linkages can be modelled in different ways. The major part of the stator flux crosses the air gap and flows into the rotor. A small part of the stator flux does not link up with the rotor winding, but constitutes the stator leakage flux. Similarly, the rotor flux can be divided into two parts: the main flux crossing the air gap and the rotor leakage flux. Mathematically, the flux linkages can be written as

$$\begin{aligned} \boldsymbol{\psi}_\mathrm{s} &= \boldsymbol{\psi}_{\mathrm{s}\sigma} + \boldsymbol{\psi}_\mathrm{m} = L_{\mathrm{s}\sigma}\boldsymbol{i}_\mathrm{s} + L_\mathrm{m}\boldsymbol{i}_\mathrm{m} \\ \boldsymbol{\psi}_\mathrm{r} &= \boldsymbol{\psi}_{\mathrm{r}\sigma} + \boldsymbol{\psi}_\mathrm{m} = L_{\mathrm{r}\sigma}\boldsymbol{i}_\mathrm{r} + L_\mathrm{m}\boldsymbol{i}_\mathrm{m} \end{aligned} \tag{2.7}$$

where $\boldsymbol{\psi}_{\mathrm{s}\sigma}$ and $\boldsymbol{\psi}_{\mathrm{r}\sigma}$ are the stator and rotor leakage flux linkages, respectively, and $\boldsymbol{\psi}_\mathrm{m}$ is the main flux. The magnetizing current is $\boldsymbol{i}_\mathrm{m} = \boldsymbol{i}_\mathrm{s} + \boldsymbol{i}_\mathrm{r}$. The magnetizing inductance is denoted by L_m, and the stator and rotor leakage inductances by $L_{\mathrm{s}\sigma}$ and $L_{\mathrm{r}\sigma}$, respectively. The stator inductance is defined as $L_\mathrm{s} = L_{\mathrm{s}\sigma} + L_\mathrm{m}$ and the rotor inductance is $L_\mathrm{r} = L_{\mathrm{r}\sigma} + L_\mathrm{m}$. Using (2.4), (2.5), and (2.7), the induction machine can be described by the T-equivalent circuit shown in Fig. 2.1(a). This model is relatively simple and gives a good description of the basic principles of the induction machine.

The T-model is, however, over-parameterized, i.e., a model with less parameters is sufficient (Slemon, 1989). Furthermore, the division of the leakage inductance into the stator leakage inductance and the rotor leakage inductance is in practice impossible based on the measurement data available during the self-commissioning of the drive. Therefore, the inverse-Γ or Γ models are often used in control applications. In the inverse-Γ model, the leakage inductance is totally referred to the stator side, the equivalent circuit of this model is shown in Fig. 2.1(b), and in the Γ model, the leakage inductance is referred to the rotor side as shown in the equivalent circuit in Fig. 2.1(c).

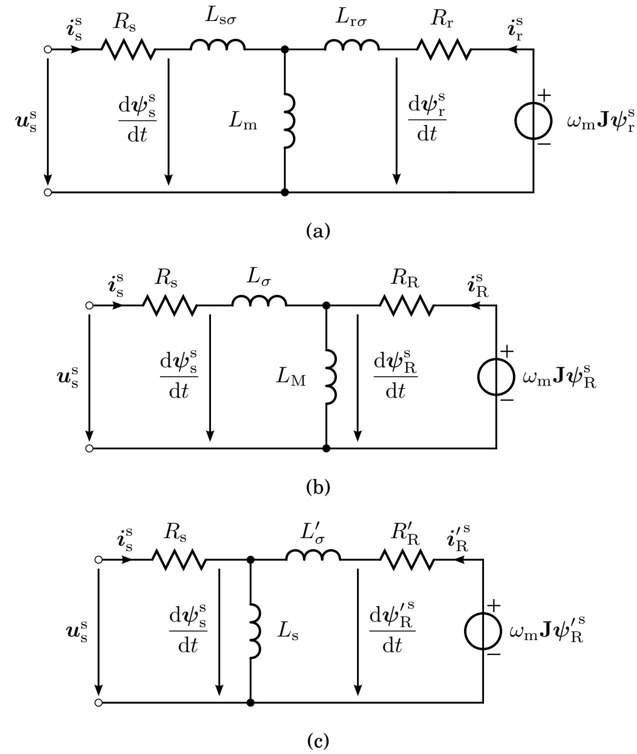

Figure 2.1. Dynamic induction machine models in stator coordinates: (a) T model, (b) inverse-Γ model, (c) Γ model. The superscript s denotes stator coordinates.

Table 2.1. Model conversion.

	Inverse-Γ model	Γ model
Coupling factor	$k_\mathrm{r} = L_\mathrm{m}/L_\mathrm{r}$	$k_\mathrm{s} = L_\mathrm{m}/L_\mathrm{s}$
Magnetizing inductance	$L_\mathrm{M} = k_\mathrm{r} L_\mathrm{m}$	$L'_\mathrm{M} = L_\mathrm{m}/k_\mathrm{s} = L_\mathrm{s}$
Leakage inductance	$L_\sigma = L_{\mathrm{s}\sigma} + k_\mathrm{r} L_{\mathrm{r}\sigma}$	$L'_\sigma = L_{\mathrm{s}\sigma}/k_\mathrm{s} + L_{\mathrm{r}\sigma}/k_\mathrm{s}^2$
Rotor resistance	$R_\mathrm{R} = k_\mathrm{r}^2 R_\mathrm{r}$	$R'_\mathrm{R} = R_\mathrm{r}/k_\mathrm{s}^2$
Rotor current	$\boldsymbol{i}_\mathrm{R} = \boldsymbol{i}_\mathrm{r}/k_\mathrm{r}$	$\boldsymbol{i}'_\mathrm{R} = k_\mathrm{s}\boldsymbol{i}_\mathrm{r}$
Rotor flux linkage	$\boldsymbol{\psi}_\mathrm{R} = k_\mathrm{r}\boldsymbol{\psi}_\mathrm{r}$	$\boldsymbol{\psi}'_\mathrm{R} = \boldsymbol{\psi}_\mathrm{r}/k_\mathrm{s}$

The parameters and the rotor quantities of the inverse-Γ and Γ models can be obtained from the parameters and rotor quantities of the T-model according to the equations in Table 2.1. The stator and rotor fluxes of the inverse-Γ model can be written as

$$\begin{aligned} \boldsymbol{\psi}_\mathrm{s} &= L_\sigma \boldsymbol{i}_\mathrm{s} + L_\mathrm{M}\boldsymbol{i}_\mathrm{M} \\ \boldsymbol{\psi}_\mathrm{R} &= L_\mathrm{M}\boldsymbol{i}_\mathrm{M} \end{aligned} \tag{2.8}$$

where the magnetizing current $\boldsymbol{i}_\mathrm{M} = \boldsymbol{i}_\mathrm{s} + \boldsymbol{i}_\mathrm{R}$. The corresponding expressions for the Γ model are

$$\begin{aligned} \boldsymbol{\psi}_\mathrm{s} &= L_\mathrm{s}\boldsymbol{i}'_\mathrm{M} \\ \boldsymbol{\psi}'_\mathrm{R} &= L_\mathrm{s}\boldsymbol{i}'_\mathrm{M} + L'_\sigma \boldsymbol{i}'_\mathrm{R} \end{aligned} \tag{2.9}$$

where the magnetizing current $\boldsymbol{i}'_\mathrm{M} = \boldsymbol{i}_\mathrm{s} + \boldsymbol{i}'_\mathrm{R}$. The inverse-Γ model is a convenient choice in vector control applications, as it leads to rather simple equations for the control of the electromagnetic torque and the rotor flux.

3. Magnetic Saturation

3.1 Magnetic Saturation Models

The most simple induction machine model naturally includes only constant-valued parameters. Such a model is sufficient to describe the fundamental-wave characteristics of the induction machine model in a certain operating point. As the operating point varies, the parameters of the machine vary due to variations in the flux magnitude and frequency. At low flux values, the inductances remain constant, but as the flux increases the machine starts to saturate and the inductances decrease. The iron losses depend both on the flux magnitude and on the frequency. The control performance can be improved by including these phenomena. The modelling of magnetic saturation and identification of the inductances will be discussed in this chapter, and the modelling of iron losses in Chapter 4.

The induction machine is usually designed to be slightly saturated in the rated operating point in order to maximize the torque production for a given machine frame (Slemon, 1989). The stator and rotor teeth have the highest flux density and are the parts where saturation mainly occurs. The flux density in the yoke is lower, but saturation might occur also in this part. The teeth and the yoke all belong to the main flux path, and it is evident that the magnetizing inductance saturates as the main flux becomes high enough.

The saturation characteristics depend on the geometrical dimensions of the machine. Small machines usually have skewed rotor slots in order to reduce cogging torques and harmonic torques. Gerada et al. (2007) studied the influence of rotor skewing on the magnetic saturation. Due to skewing, the flux is reduced at one end of the machine and increased at the other end. Because of saturation, the reduction is larger than the increase and the overall flux is lower than it would be without skewing the rotor slots. The effect is aggravated as the load increases, leading to a load dependency of the main flux. If the rotor slots are closed, the rotor leakage flux flows partly through the saturating rotor bridges. The rotor leakage inductance becomes heavily nonlinear as a result (Williamson and Begg, 1985), but the closed rotor slots also affect the main flux that is almost perpendicular to the rotor leakage flux and crosses the leakage flux at the rotor surface (Yahiaoui and Bouillault, 1995). Nerg et al. (2004) studied the load-dependency of the magnetizing inductance using finite element analysis and observed that the inductance decreases as the torque increases.

3.2 Models Including the Saturation of the Main Flux Path

The magnetic saturation affects the inductances of the machine, i.e., the inductances vary as a function of the operating point. As a result, the relationship between the steady-state voltages and currents varies. Usually, only the saturation in the main flux path is taken into account in induction machine models intended for the control of the machine. The saturation curve can be modeled in various ways. de Jong (1980) proposed a power function for the modeling of the saturation curve. The magnitude of the main flux can be written as

$$\psi_{\mathrm{m}} = \frac{L_{\mathrm{mu}} i_{\mathrm{m}}}{1 + (\alpha \psi_{\mathrm{m}})^S} \tag{3.1}$$

where L_{mu} is the unsaturated value of the magnetizing inductance, i_{m} is the magnetizing current, ψ_{m} is the main flux linkage magnitude, and α and S are non-negative parameters. The saturation can also be modeled by polynomial functions (Kerkman, 1985), the hyperbolic tangent function (Coussens et al., 1994) or simply by look-up tables. Soft-computing techniques, such as the neural network, have also been proposed for storing the inductance values (Wlas et al., 2008).

Models including the saturation have gained a lot of interest for many years. Boldea and Nasar (1988) presented a general circuit including the main flux saturation as well as the skin effect of the rotor. As an alternative to the T-model, Sullivan and Sanders (1995) developed a π-model that includes the saturation of the stator and rotor teeth. Levi (1997) used the idea of a generalized flux for the modelling of the magnetic saturation, and showed that different sets of state-space variables can be used in the model.

The influence of the saturation can also be seen in the dynamic response, which was investigated by Melkebeek and Novotny (1983) using a linearized small-signal model. Assuming that saturation occurs only in the magnetizing branch, two inductances were used to describe the relationship between the magnetizing current and the main flux: the operating-point inductance (or chord-slope inductance) L_{m0} and the incremental inductance (or transient inductance) L_{mt0}. If the magnitude of the magnetizing current varies, the change in the main flux magnitude depends on the level of saturation. The relationship between the magnetizing current magnitude and flux magnitude can be described by the tangent of the saturation curve, i.e., the transient inductance. The operating-point inductance, on the other hand, relates the main flux response to variations in the angle of the magnetizing current. The deviations in the main flux can be described as

$$\begin{bmatrix} \tilde{\psi}_{\mathrm{md}} \\ \tilde{\psi}_{\mathrm{mq}} \end{bmatrix} = \boldsymbol{L}_{\mathrm{m}} \begin{bmatrix} \tilde{i}_{\mathrm{md}} \\ \tilde{i}_{\mathrm{mq}} \end{bmatrix} \tag{3.2}$$

where the inductance matrix is

$$\begin{aligned} \boldsymbol{L}_{\mathrm{m}} &= \begin{bmatrix} L_{\mathrm{mdd}} & L_{\mathrm{mdq}} \\ L_{\mathrm{mqd}} & L_{\mathrm{mqq}} \end{bmatrix} = \mathrm{e}^{\mathbf{J}\vartheta_{\mathrm{m0}}} \begin{bmatrix} L_{\mathrm{mt0}} & 0 \\ 0 & L_{\mathrm{m0}} \end{bmatrix} \mathrm{e}^{-\mathbf{J}\vartheta_{\mathrm{m0}}} \\ &= \begin{bmatrix} L_{\mathrm{mt0}}\cos^2(\vartheta_{\mathrm{m0}}) + L_{\mathrm{m0}}\sin^2(\vartheta_{\mathrm{m0}}) & (L_{\mathrm{mt0}} - L_{\mathrm{m0}})\sin(\vartheta_{\mathrm{m0}})\cos(\vartheta_{\mathrm{m0}}) \\ (L_{\mathrm{mt0}} - L_{\mathrm{m0}})\sin(\vartheta_{\mathrm{m0}})\cos(\vartheta_{\mathrm{m0}}) & L_{\mathrm{m0}}\cos^2(\vartheta_{\mathrm{m0}}) + L_{\mathrm{mt0}}\sin^2(\vartheta_{\mathrm{m0}}) \end{bmatrix} \end{aligned} \tag{3.3}$$

The angle of the operating-point magnetizing current is denoted by ϑ_{m0}. In the case of no saturation, $L_{\mathrm{mt0}} = L_{\mathrm{m0}}$, and the inductance matrix $\boldsymbol{L}_{\mathrm{m}} = L_{\mathrm{m0}}\mathbf{I}$. As the machine saturates, $L_{\mathrm{mdd}} \neq L_{\mathrm{mqq}}$, i.e., the saturation induces saliency in transients. The flux response to variations in the d-direction current is then different from the flux response to variations in the q-direction current. The phenomenon is referred to by many authors as cross saturation. The location of the saliency can be measured by signal injection (Aime et al., 1998). Knowledge of the location could be useful for estimation of the flux position in sensorless drives, but a more detailed model is then necessary, as the saturation does not only occur in the magnetizing path and the saliency is not necessarily fixed to the main flux as predicted by the model above.

3.3 Advanced Saturation Models

Ojo et al. (1990) presented a model where the saturation in the stator and rotor cores is modeled separately from the saturation in the stator and rotor teeth. Saturation factors relating the saturated parameters to the saturated parameters were used in the model. The identification of the model was based on search coils inside the machine and finite element analysis, and the model is thus not suitable for control purposes. Healey et al. (1995) included the saturation of the main flux path as well as the saturation of the rotor leakage flux path in the motor model. The main flux was assumed to be dependent on the magnetizing current and the rotor leakage inductance dependent on the rotor current. Proca and Keyhani (2002) proposed an induction machine model, where the magnetizing inductance was dependent on the flux-producing component of the stator current and the leakage inductance was dependent on the total current. Polynomial functions were used to model the variation of the inductances. A model including both magnetic saturation and the skin effect of the rotor was proposed by Sudhoff et al. (2002). The leakage inductances were modeled as dependent on the stator and rotor currents as well as the main flux. The magnetizing inductance was modeled as a function of the magnetizing current.

Tuovinen et al. (2010) proposed explicit functions for the dependency of the main flux and the leakage flux on the magnetizing and rotor currents. The mutual saturation between the main flux and the leakage flux was included in the model. This kind of model could give a very good accuracy in various operating points with different flux and torque values. The difficulty is to identify all necessary parameters. Tuovinen et al. (2010) applied data fitting based on data from a large number of operating points. This method is useful in a laboratory environment where the load as well as the speed can be varied freely. In a real-life application, the load cannot be controlled and therefore the identification is more difficult.

Soft computing techniques for modeling nonlinear systems have also been developed. One of these is the neural network that was proposed for the modeling of the induction machine by Moon et al. (1999). In this model, all parameters are allowed to vary and the neural network can basically model any phenomenon that has to be included in the control of the drive. However, the neural network needs a lot of training data in order to model the system correctly. For the training of the network, Moon et al.

(1999) used an input pattern that was based on the data from an acceleration test where the speed is measured, and an output pattern based on a maximum likelihood estimation. The input pattern included a lot of data at very high slip levels and only a few points at low slip levels. As the induction machine normally is controlled to have a relatively low slip, the training data is not very good for the purpose of control of the drive.

3.4 Proposed Small-Signal Model

In order to include the saturation in the rotor leakage path and the mutual saturation between the main flux path and the rotor leakage flux path, a small-signal model was developed in Publication V. The magnetizing inductance is assumed to be dependent on the magnetizing current and the rotor current according to

$$L_{\mathrm{m}}(i_{\mathrm{m}}, i_{\mathrm{r}}) = \frac{\psi_{\mathrm{m}}(i_{\mathrm{m}}, i_{\mathrm{r}})}{i_{\mathrm{m}}} \tag{3.4}$$

Similarly, the rotor leakage inductance is assumed to be a function of the rotor current and magnetizing current

$$L_{\mathrm{r}\sigma}(i_{\mathrm{m}}, i_{\mathrm{r}}) = \frac{\psi_{\mathrm{r}\sigma}(i_{\mathrm{m}}, i_{\mathrm{r}})}{i_{\mathrm{r}}} \tag{3.5}$$

Hence, the influence of the torque on the saturation characteristics is included in the model. The incremental inductances are defined as

$$\begin{aligned} L_{\mathrm{mt}}(i_{\mathrm{m}}, i_{\mathrm{r}}) &= \frac{\partial\psi_{\mathrm{m}}(i_{\mathrm{m}}, i_{\mathrm{r}})}{\partial i_{\mathrm{m}}}, \quad L_{\mathrm{r}\sigma\mathrm{t}}(i_{\mathrm{m}}, i_{\mathrm{r}}) = \frac{\partial\psi_{\mathrm{r}\sigma}(i_{\mathrm{m}}, i_{\mathrm{r}})}{\partial i_{\mathrm{r}}}, \\ L_{\mathrm{t}}(i_{\mathrm{m}}, i_{\mathrm{r}}) &= \frac{\partial\psi_{\mathrm{m}}(i_{\mathrm{m}}, i_{\mathrm{r}})}{\partial i_{\mathrm{r}}} = \frac{\partial\psi_{\mathrm{r}\sigma}(i_{\mathrm{m}}, i_{\mathrm{r}})}{\partial i_{\mathrm{m}}} \end{aligned} \tag{3.6}$$

where the last equality follows from the reciprocity condition. The reciprocity condition ensures that losses are not unintentionally included in the model.

Due to the rotor leakage inductance saturation and the mutual saturation effect, the saliency is not fixed only to the main flux. The location of the saliency depends on the operating point. In the case of no load, the rotor current is zero and the saliency is fixed to the main flux. As the load increases, the influence of the rotor leakage saturation increases, and the location of the saliency depends on the rotor leakage flux as well as the main flux.

The saturation-induced saliency has been used to identify the position of the flux (Jansen and Lorenz, 1996; Blaschke et al., 1996). The proposed small-signal model could, at least in theory, be used for this purpose if all parameters were known, and the result would be more accurate than if the model by Melkebeek and Novotny (1983) were used. However, the identification of all parameters is difficult. In a laboratory environment, the parameters can be found in different operating points using data fitting, as demonstrated in Publication I and Publication V.

3.5 Inductance Identification

The traditional methods for identifying the electrical parameters of the induction machine are the no-load and locked-rotor tests. In a no-load condition, the stator current flows through the magnetizing branch, and the rotor current is zero. Based on the stator voltage and stator current, the stator inductance can, thus, rather easily be obtained. If the measurements are performed at several stator voltage magnitudes, the magnetizing curve can be obtained. When the rotor is locked, the major part of the current flows through the rotor branch and the leakage inductance can be identified.[1] However, in real-life applications, the no-load and locked-rotor tests are not always applicable. Ideally, the self-commissioning of a drive is performed at standstill, and the no-load test which requires the machine to run at synchronous speed might not be possible. However, a more accurate estimate of the magnetizing inductance can be obtained if the machine is allowed to run during the identification process. Locking the rotor requires a lot of work and might even be impossible. Furthermore, the variation of the parameters as the torque varies cannot be predicted by the no-load and locked rotor tests, and the leakage inductance obtained in a locked-rotor test is affected by the deep bar effect. Therefore, numerous identification methods have been developed to overcome these problems.

Identification of the Magnetizing Inductance

The machine can be ensured to remain at standstill by using only single-phase excitation. One method proposed to identify the magnetizing inductance using single-phase excitation is to analyze the voltage and current

[1] The leakage inductance seen from the stator terminals corresponds to the leakage inductance of the inverse-Γ model. If the magnetizing inductance L_{M} is known, the leakage inductance of the Γ model can be obtained as $L'_\sigma = (L_\sigma/L_{\mathrm{M}})(L_\sigma + L_{\mathrm{M}})$.

during the reversal of the flux direction. A constant DC voltage is applied at the stator terminals in order to build up magnetic flux of a constant magnitude. The direction of the flux is then reversed by reversing the voltage. Sumner and Asher (1993) used a recursive least squares algorithm to extract the rated magnetizing inductance. Rasmussen et al. (1996) and Sukhapap and Sangwongwanich (2002) identified the magnetizing curve based on integration of the voltage data from the flux reversal. The leakage inductance seen from the stator terminals affects the fast transients of the machine and might cause inaccurate results. In the proposed methods, the first data points of the measured voltages and currents have to be removed to reduce the influence of the leakage inductance.

Another method for obtaining the magnetizing inductance is to use a sinusoidal voltage at a low frequency. Klaes (1993) proposed an iterative identification procedure, where both the magnetizing inductance and the leakage inductance are obtained. The identification is based on the Γ model, and it is assumed that the magnetizing inductance is dependent only on the stator flux and the leakage inductance only on the stator current. A number of measurements covering the desired flux region are performed at a very low frequency, assuming that the magnetizing inductance dominates the current response and the influence of leakage inductance estimate errors is small. Correspondingly, measurements with a higher frequency are used to obtain the leakage inductance estimate. Gastli (1999) also used measurements at two frequencies to determine the parameters. The impedance seen at the stator terminals was measured at both frequencies, and the parameters of the T-, Γ, and inverse-Γ equivalent circuits were determined based on the impedance. The parameters of the inverse-Γ equivalent circuit were obtained with satisfactory accuracy after applying an additional recursive algorithm for the magnetizing inductance estimation. The accuracy of the parameters of the T- and Γ circuits was poor.

Bünte and Grotstollen (1993) used a motor model where the saliency induced by the saturation of the magnetizing path is included. A linearized small-signal model was developed for the identification of machine parameters. By measuring the current response at multiple frequencies at standstill and using a least-square algorithm for data fitting, all electrical parameters of the machine were obtained.

Levi and Vukosavic (1999) proposed an identification method of the magnetizing curve. A function based on the stator current and stator voltage integral was utilized in the identification. The method requires the machine to run at a low speed without load during the identification, and the leakage inductance and the rated rotor time constant have to be known.

Bertoluzzo et al. (2001) used a polynomial function for modeling of the inverse-Γ main flux as a function of the magnetizing current. The machine was supplied with a low-frequency single-phase voltage, and the stator voltage and stator current were measured. The parameters of the saturation function were obtained using a recursive least-squares algorithm. The reference value for the identification algorithm was calculated by high-pass filtering the rotor flux obtained from the voltage model. The stator resistance and leakage inductance were assumed to be known.

Identification of the Leakage Inductance

Several methods for the identification of the leakage inductance based on transients have been proposed. Schierling (1988) proposed a method where the leakage inductance is determined based on the initial current response as a voltage pulse is applied. Errors due to the skin effect and eddy current effect in the iron were compensated for by fitting an exponential function to the measured current, and the inductance was calculated using the fitted curve instead of the measured current. Sukhapap and Sangwongwanich (2002) also used a voltage pulse, but the leakage inductance was obtained by using a recursive least-squares algorithm.

Sumner and Asher (1993) proposed a method where a single-phase constant voltage was fed into the machine and a pseudo-random binary sequence (PRBS) voltage was superimposed on the constant voltage. The stator leakage inductance was obtained based on the voltage and current using a recursive least squares algorithm.

Kerkman et al. (1996) compared frequency-based techniques to the transient-based methods. A single-phase voltage excitation at several frequencies was used, and the leakage inductance was obtained by analyzing the impedance. The results showed that the frequency-based test gives better results than the voltage-pulse test.

Holliday et al. (1994) proposed an online identification method of the leakage inductance. High-frequency signal injection was used to mimic the conditions of a locked-rotor test. A rotating voltage signal was superimposed on the fundamental wave, and the corresponding current is extracted in order to obtain the impedance. As the identification is performed online, the influence of the load can be observed. The method does not take the saturation-induced saliency into account, however.

Zamora and García-Cerrada (2000) proposed a method for the identification of the stator inductance, leakage inductance, and stator resistance during the operation of the drive. The identification was based on the fundamental-wave stator currents and voltages. Three different operating point areas were defined for the identification of each of the parameters. The areas were chosen based on the sensitivity of the parameter to be identified on the other parameters. The stator inductance was thus identified at low load, and the leakage inductance was identified at high load. The method cannot simultaneously identify the influence of the load on the leakage and stator inductances. Furthermore, there is no way to obtain the leakage inductance at low loads or low speeds.

3.6 Proposed Identification Methods

Identification of the Leakage Inductance

Due to the load-dependency of the rotor leakage inductance, the identification should be performed online in order to achieve a good accuracy in all operating points. An identification method based on signal injection was proposed in Publication II, where voltage signal injection was used. A similar approach was used in Publication VIII, where current signal injection was applied. The identification is based on a reduced-order small-signal model presented in Publication V. At higher excitation frequencies, the impedance seen at the stator terminals can be written as

$$\boldsymbol{Z}_{\mathrm{s}} = \boldsymbol{R}_{\sigma} + (s\mathbf{I} + \omega_{\mathrm{s0}}\mathbf{J})\boldsymbol{L}_{\sigma} \tag{3.7}$$

where $\boldsymbol{R}_{\sigma}$ is the total resistance matrix and $\boldsymbol{L}_{\sigma}$ is the total leakage inductance matrix. The impedance can be measured in any operating point using signal injection. Due to the saturation-induced saliency, the measured resistance and inductance depend on the reference frame. Denoting the inductance matrix by

$$\boldsymbol{L}_{\sigma} = \begin{bmatrix} L_{\mathrm{dd}} & L_{\mathrm{dq}} \\ L_{\mathrm{qd}} & L_{\mathrm{qq}} \end{bmatrix}, \tag{3.8}$$

the saliency can be studied by observing the variation of an inductance matrix element as the reference frame is varying. Based on the leakage

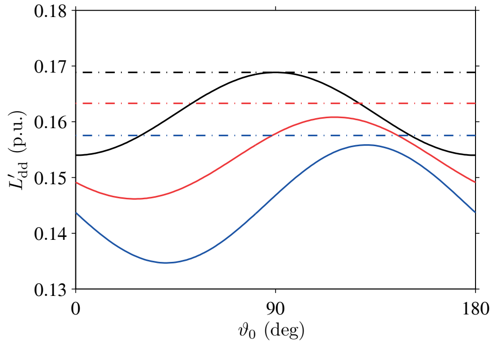

Figure 3.1. Leakage inductance as a function of the angle of the reference frame. $\vartheta_0 = 0$ corresponds to a reference frame aligned with the rotor flux. The inductance is shown at rated load (blue curve), half of rated load (red curve), and no load (black curve). The stator flux is 0.9 p.u.

inductance matrix $\boldsymbol{L}_\sigma$ in a reference frame aligned with the rotor flux, the leakage inductance in different reference frames can be obtained from the coordinate transformation

$$\boldsymbol{L}'_\sigma = \begin{bmatrix} L'_{dd} & L'_{dq} \\ L'_{qd} & L'_{qq} \end{bmatrix} = e^{-\mathbf{J}\vartheta_0} \boldsymbol{L}_\sigma e^{\mathbf{J}\vartheta_0} \tag{3.9}$$

similarly to (3.3). As an example, the matrix element L'_{dd} predicted by the model is shown as a function of the reference frame angle in Fig. 3.1 in a few operating points. The operating-point total leakage inductance is also shown in each case. The data for Fig. 3.1 was obtained from the experimental data of a 2.2-kW machine presented by Tuovinen et al. (2010). The definition of the reference frame angle is illustrated in Fig. 3.2. In a no-load condition, saturation only occurs in the main flux path, and the saliency is fixed to the direction of the magnetizing current vector. The maximum of L_{dd} then occurs as the angle of the magnetizing current is $90°$ (or $-90°$). As the load increases, the rotor branch saturates and the saliency is dependent also on the direction of the rotor current. As a result, the inductance curve is shifted horizontally. The curve is also shifted downwards as the inductances decrease due to the saturation.

The maximum value of the observed small-signal inductance L_{dd} can be used as the estimate for the operating-point leakage inductance. As illustrated in Fig. 3.1, the maximum value is very close to the desired total leakage inductance in most operating points. The influence of the main flux saturation on the accuracy of the estimated inductance was discussed in Publication II. The largest errors occur when the machine is driven into deep saturation and the rotor leakage inductance is of the

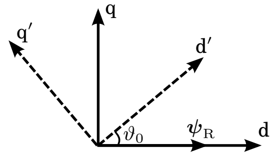

Figure 3.2. Reference frames used when calculating L'_{dd}. The dq-reference frame is aligned with the rotor flux. The element L'_{dd} is evaluated in the d′q′-reference frame.

same magnitude as the incremental magnetizing inductance. This situation might occur at rated or higher flux levels and low load torque levels in machines where the rotor leakage inductance increases drastically as the load torque approaches zero.

Identification of the Stator Inductance

An identification method for the stator inductance was proposed in Publication VIII. The stator inductance can in a no-load condition be modeled as

$$L_s(\psi_s) = \frac{L_{su}}{1 + (\beta\psi_s)^S} \tag{3.10}$$

and adaptation laws can be applied during the self-commissioning of the drive in order to obtain the parameters L_{su} and β. As the parameter S can be chosen based on a priori information, the entire magnetizing curve is known after the adaptation process is completed. If the stator inductance identification method is combined with the leakage inductance identification method, the magnetizing inductance of the inverse-Γ model can be calculated as $L_M = L_s - L_\sigma$.

The expression for the stator inductance in (3.10) does not include the influence of the load. As the load torque increases, the stator inductance decreases even though the stator flux is controlled to be constant. Taking the influence of the load into account, the stator inductance can be modeled as (Tuovinen et al., 2010)

$$L_s = \frac{L_{su}}{1 + (\beta\psi_s)^S + \frac{\gamma L_{su}}{d+2}\psi_s^c \psi_\sigma'^{d+2}} \tag{3.11}$$

This equation includes six parameters (L_{su}, β, S, γ, c, and d), and the identification of all parameters is very difficult in real-time applications.

The sensitivity of the stator inductance estimate to errors in the leakage inductance estimate can be formulated as (Zamora and García-Cerrada,

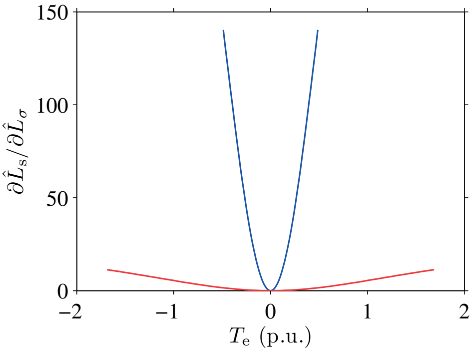

Figure 3.3. Sensitivity of the stator inductance estimate to errors in the leakage inductance estimate. The rotor flux $\psi_R = 0.9$ p.u. (red curve) and $\psi_R = 0.3$ p.u. (blue curve). The stator angular frequency is 1 p.u.

2000)

$$\frac{\partial \hat{L}_s}{\partial \hat{L}_\sigma} = \frac{(u_{s0} i_{s0})^2 - (\boldsymbol{u}_{s0}^T \mathbf{J} \boldsymbol{i}_{s0})^2 + (R_s i_{s0}^2)^2 - 2R_s i_{s0}^2 \boldsymbol{u}_{s0}^T \boldsymbol{i}_{s0}}{(\boldsymbol{u}_{s0}^T \mathbf{J} \boldsymbol{i}_{s0})^2 - 2\omega_{s0} L_\sigma i_{s0}^2 \boldsymbol{u}_{s0}^T \mathbf{J} \boldsymbol{i}_{s0} + (L_\sigma \omega_{s0} i_{s0}^2)^2} \tag{3.12}$$

The sensitivity for the 2.2-kW machine is shown in Fig. 3.3 for two different levels of the rotor flux. At low flux levels, the stator inductance estimate is much more sensitive to errors in the leakage inductance estimate than at higher flux levels. In other words, the identification of the parameter L_{su}, which is obtained at low flux levels, requires a more accurate estimate of the leakage inductance than the identification of the parameter β, which can be identified at higher flux levels. The sensitivity to errors in the leakage inductance is independent of the stator frequency.

The accuracy of the stator inductance estimate is also affected by the accuracy of the stator resistance estimate. The sensitivity to errors in the stator resistance is

$$\frac{\partial \hat{L}_s}{\partial \hat{R}_s} = \frac{2\hat{R}_s i_{s0}^4 - 2\omega_{s0} \boldsymbol{u}_{s0}^T \boldsymbol{i}_{s0} \boldsymbol{u}_{s0}^T \mathbf{J} \boldsymbol{i}_{s0} - \hat{L}_\sigma \omega_{s0}^2 i_{s0}^4}{(\omega_{s0} \boldsymbol{u}_{s0}^T \mathbf{J} \boldsymbol{i}_{s0} - \hat{L}_\sigma \omega_{s0} i_{s0}^2)^2} \tag{3.13}$$

The sensitivity is illustrated in Fig. 3.4. The stator inductance is much less sensitive to errors in the stator resistance estimate than to errors in the leakage inductance estimate. The sensitivity also depends on whether the torque is positive or negative. A stator resistance estimate that is too small reduces the stator inductance estimate when the torque is negative, while the stator inductance estimate increases when the torque is positive. The stator angular frequency in Fig. 3.4 is 1 p.u. The sensitivity increases as the frequency decreases.

The iron losses have not been included in the analysis above. According to simulations, inaccuracies in the iron loss model have a similar influence

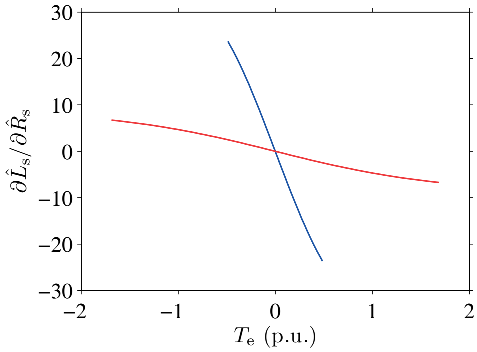

Figure 3.4. Sensitivity of the stator inductance estimate to errors in the stator resistance estimate. The rotor flux $\psi_R = 0.9$ p.u. (red curve) and $\psi_R = 0.3$ p.u. (blue curve). The stator angular frequency was 1 p.u.

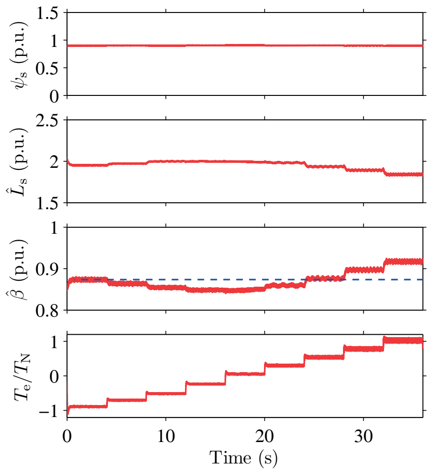

Figure 3.5. Experimental results of the stator inductance adaptation as the load torque is varied stepwise from negative rated torque to positive rated torque. The speed is 0.75 p.u., the rotor flux is 0.8 p.u., and $L_{su} = 2.31$ p.u.

on the stator inductance estimate as the stator resistance, i.e., the error depends on whether the torque is positive or negative. Inaccuracies in the modeling of inverter delays can also affect the results of the inductance identification. As an example, the adaptation of the stator inductance as the torque is varied and the iron losses are omitted in the induction machine model is shown in Fig. 3.5. The stator inductance decreases as the load increases, and the decrease in the stator inductance is much larger as the torque is positive than in the case of a negative torque.

4. Iron Losses and the Deep Bar Effect

Iron losses are usually divided into hysteresis losses and eddy current losses. The origin of the hysteresis losses can be explained by the domain theory. As a ferromagnetic material is exposed to a magnetic field, the magnetic domain walls transfer and rotate, and this process requires energy. Eddy currents, on the other hand, arise as a result of electric fields induced by the varying magnetic field. Hysteresis losses are proportional to the frequency, while the eddy current losses are commonly modeled as proportional to the square of the frequency. In some cases, excess losses are also included in iron loss models in order to achieve a better agreement between measurement results and losses predicted by the model. The inclusion of excess losses might be necessary, especially at high flux densities and high frequencies.

Iron losses occur both in the stator and the rotor of the induction machine. As the stator frequency is much higher than the slip frequency, the major part of the iron losses takes place in the stator. A pulse-width modulation (PWM) waveform includes high frequencies causing increasing losses in the rotor. Eddy currents develop in the rotor bars, and as a result, the effective rotor resistance increases while the rotor leakage inductance decreases. This skin effect phenomenon is pronounced in machines equipped with deep rotor bars. According to Laldin et al. (2011), core losses might be also induced in the rotor by motion harmonics.

When it comes to the accuracy of the control, the fundamental-wave losses are the most important. Hence, it is typically sufficient to model only the iron losses of the stator. Levi et al. (1996) used a model where the iron loss resistance was placed in parallel to the magnetizing branch to study the influence of the iron losses on the control accuracy. The iron loss resistance was modeled as a function of the frequency, and the identification was based on no-load measurements. It was observed that the

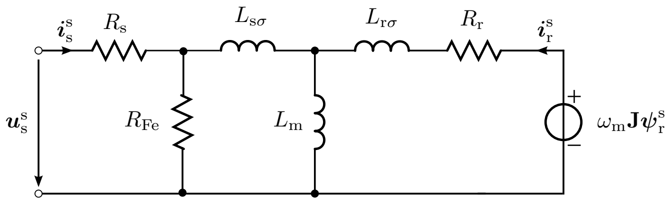

Figure 4.1. Dynamic T model in stator coordinates with iron loss resistance in parallel to the stator inductance $L_{s\sigma} + L_m$.

omission of iron losses in the control algorithms can cause detuning of torque and rotor flux, especially at the rated speed, and the inaccuracy might be even more severe in the flux-weakening region. Modeling of the fundamental-wave losses is important also when applying loss-minimizing control algorithms as in Publication VII. The inclusion of the skin effect becomes necessary when analyzing the high-frequency response of the machine. In control applications, a typical example is the identification of parameters based on high-frequency excitation. The skin effect should be included in the model particularly if the machine is equipped with deep bars. In some cases, the skin effect of the rotor bars need to be modeled also in order to improve the accuracy of the fundamental-wave control (White and Hinton, 1995).

4.1 Iron Loss Models

Typically, the stator iron losses are included in the model of the machine by placing a resistance in parallel to the stator inductance as in Fig. 4.1, or in parallel to the magnetizing inductance. The resistor is often constant-valued, and the frequency characteristics of the resulting iron losses correspond to the eddy current losses. Boldea and Nasar (1987) added an inductor in series with the resistor in order to model the rate of change of eddy current losses.

The problem of modeling the hysteresis losses has been addressed by many authors. Chua and Stromsmoe (1970) presented a model for the iron losses of nonlinear inductors. The losses were modeled by a dissipating function, while the saturation characteristics were modeled separately from the losses by a restoring function. In a lumped-circuit model, the model by Chua and Stromsmoe (1970) corresponds to placing a nonlinear resistor in parallel to a nonlinear inductor. Conditions that the functions should fulfill were discussed. The functions were determined geometrically, but no explicit functions were given. The use of a nonlinear resistor was also proposed by Lin et al. (1989). Menemenlis (1998) developed a model for the hysteresis losses of a transformer. A saturation function was presented, and various reduction factors were used to produce minor and major loops. A piecewise linear resistance function was used by Neves and Dommel (1993).

Modeling of hysteresis losses in an electrical machine is demanding as the flux is rotating and a hysteresis curve cannot be defined in the same way as for a transformer. Shinnaka (2001) modeled the core losses of the induction machine with two parallel resistors: one constant-valued resistor for the eddy current losses and one resistor proportional to the frequency for modeling of the hysteresis losses. The model can be used for modeling of the fundamental-wave losses in steady state. During transients, the model cannot be used as the frequency cannot be determined. The model does not either take into account losses due to higher-order excitation frequencies present when using a PWM supply.

4.2 Proposed Iron Loss Model

A core loss model that can be used for the modeling of induction machines as well as inductors was proposed in Publication III and Publication VI. The model follows the ideas presented by Chua and Stromsmoe (1970). The core losses are modelled by a nonlinear resistor that can be divided into two parts, one for the eddy currents and one for the hysteresis losses. To model the eddy current losses, a constant-valued resistance R_{Ft} is sufficient. In the case of a sinusoidally varying flux linkage, the resulting core losses are proportional to the square of the frequency and the square of the flux magnitude, i.e., the losses correspond to eddy current losses. The steady-state hysteresis losses, however, are normally modeled as proportional to the frequency and proportional to the n-th power of the flux magnitude, where n is in the range $1 \dots 2$. This could be accomplished by using a resistor that is dependent on the frequency (Shinnaka, 2001), but here, a resistor of the form

$$R_{\mathrm{Hy}} = \frac{R_{\mathrm{Ft}} u}{k \psi_{\mathrm{s}}^{n-1}} \tag{4.1}$$

is proposed instead. The voltage over the resistor is $u = ||\boldsymbol{u}_{\mathrm{s}} - R_{\mathrm{s}} \boldsymbol{i}_{\mathrm{s}}||$ and k is a positive-valued parameter. As the frequency is not included in (4.1), the resistance is defined also during transients, and losses due to harmonics are automatically included. The total core losses can be modeled by the parallel coupling of R_{Ft} and R_{Hy}.

4.3 Deep Bar Effect

The skin effect can be modeled by defining functions for the rotor resistance and the rotor leakage inductance that are dependent on the excitation frequency. The variation of the rotor parameters with frequency depends on the shape of the rotor bars. For a rectangular bar shape, hyperbolic functions are obtained (Alger, 1965). These functions have been used for the skin effect modeling by Retière and Ivanès (1999) and for the identification of rotor parameters by Kwon et al. (2009).

A skin effect model that fits to any rotor bar shape can be achieved by adding rotor branches in parallel to the rotor resistance and rotor leakage inductance. The number of rotor branches added depends on the desired accuracy of the model. Measurements can be performed at a few frequencies, and the parameter values can rather easily be obtained by data fitting. The saturation of the rotor leakage inductance can be modeled separately from the skin effect. Williamson and Healey (1996) modeled the saturation by a rotor leakage inductance dependent on the rotor current, and the skin effect by two constant-valued inductors and resistors as shown in Fig. 4.2. Monjo et al. (2013) studied experimentally the deep bar model of a saturating machine for large slip variations. It was observed that leakage inductance saturation needs to included in the model in order to achieve a good agreement between the behavior predicted by the model and the measured results. The ladder circuit can be seen as a transfer function dependent on the excitation frequency. Sudhoff et al. (2002) also used a transfer function for the rotor admittance for modeling of the frequency characteristics of the rotor. However, the function was not explicitly dependent on any frequency and can, therefore, be used in time-domain models.

4.4 Proposed Model of the Deep Bar Effect

The eddy currents of the rotor bars and the rotor core are included in a model presented in Publication IV. The rotor leakage inductance is modeled by two inductors of which one is dependent on the current in order to

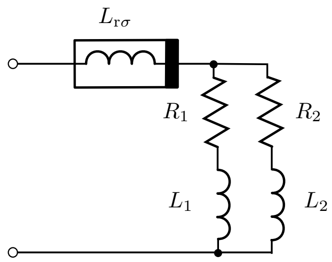

Figure 4.2. Rotor circuit model including the saturation and deep bar effect.

include the saturation. Resistances are placed in parallel with the inductors in order to include the eddy current losses. The model is used for the identification of the rotor parameters using signal injection. Using this model, the rotor leakage inductance and rotor resistance seen at zero frequency (approximately the same as the slip frequency) can be determined.

5. Summaries of Publications

The abstracts of the publications are reprinted in Section 5.1. Publication I and Publication V deal with a small-signal model of the induction machine including the effects of magnetic saturation. Based on the small-signal model, an identification method for the leakage inductance is developed in Publication II. In Publication IV, the influence of the skin effect is also taken into account in the leakage inductance identification. Publication III and Publication VI deal with the inclusion of iron losses in induction machines and nonlinear inductors. A loss-minimizing algorithm is presented in Publication VII based on the iron loss model. Publication VIII deals with the identification of the stator inductance of a saturated induction machine. Preliminary versions of Publication V, Publication VII, and Publication VIII were presented at conferences (Hinkkanen et al., 2007; Qu et al., 2011; Ranta and Hinkkanen, 2012).

5.1 Abstracts

Publication I

Due to magnetic saturation, the small-signal admittance of an induction motor is dependent on the direction of the excitation signal. The angle-dependence of the admittance can be used in the estimation of the flux angle, and it should be taken into account when identifying motor parameters. In this paper, the small-signal admittance of a 2.2-kW induction motor is measured at different excitation frequencies and operating points. The measured admittances are compared to data obtained by means of finite element analysis (FEA). A small-signal model of the induction motor is fitted to the admittances to analyze the results. The admittances obtained from FEA and laboratory experiments correspond well to each other, particularly at low excitation frequencies.

Publication II

The paper proposes an identification method for the inductances of induction machines, based on signal injection. Due to magnetic saturation, a saturation-induced saliency appears in the induction motor, and the total leakage inductance estimate depends on the angle of the excitation signal. The proposed identification method is based on a small-signal model that includes the saturation-induced saliency. Because of the saturation, the load also affects the estimate, and measurements are needed in different operating points. Using the identified total leakage inductance, an estimate of the stator inductance can be obtained. The identification method is applied to computer simulations and laboratory experiments of a 2.2-kW induction motor.

Publication III

This paper proposes a method for including both hysteresis losses and eddy current losses in the dynamic space vector model of induction machines. The losses caused by the rotation and magnitude changes of the flux vector are taken into account. The model can be applied, for example, to time-domain simulations and real-time applications such as drive control. Finite element analysis, simulations, and laboratory experiments of a 45-kW motor are used for the investigation. It is shown that the model can predict the iron losses in a wide frequency range. The accuracy is significantly improved as compared to earlier models.

Publication IV

An induction machine model is proposed for the identification of rotor parameters using high-frequency signal injection. The model includes both the magnetic saturation caused by the fundamental-wave components and the frequency dependence encountered in the signal injection method. Both the skin effect in the rotor winding and the eddy current losses in the rotor core are taken into account. Sinusoidal signal injection is used at several frequencies, and the model parameters are fitted to the results. The rotor leakage inductance and the rotor resistance valid at low slip frequencies are also obtained from the model directly. Experimental results for a 45-kW machine are presented. It is shown that the model fits well to the measured data in various operating points, and the accuracy of the identified parameters is good.

Publication V

A small-signal model is derived for saturated induction machines. Inductances are allowed to saturate as a function of their own current (or flux), and the mutual saturation effect originating mainly from skewed or closed rotor slots is also included in the model. The model fulfills the reciprocity conditions, and it can be applied to parameter identification and to the analysis and development of flux-angle estimation methods. As application examples, the parameters of a 2.2-kW induction machine were identified using the data obtained from time-stepping finite-element analysis and locked-rotor measurements. The proposed model fits well to the data, and the fitted parameters are physically reasonable.

Publication VI

A time-domain model including the core losses of a nonlinear inductor is proposed. The model can be seen as a parallel combination of a nonlinear inductance modelling the saturation and a nonlinear resistance modelling the core losses. The desired steady-state core-loss profile is used to determine the resistance function. The model is easy to implement and can be used in many different applications. The hysteresis loop of an electrical steel sample is measured at several frequencies in order to experimentally verify the model. It is shown that the model is able to predict both major and minor hysteresis loops very well.

Publication VII

This paper applies a dynamic space-vector model to loss-minimizing control in induction motor drives. The induction motor model, which takes hysteresis losses and eddy-current losses as well as the magnetic saturation into account, improves the flux estimation and rotor-flux-oriented control. Based on the corresponding steady-state loss function, a method is proposed for solving the loss-minimizing flux reference at each sampling period. A flux controller augmented with a voltage feedback algorithm is applied for improving the dynamic operation and field weakening. Both the steady-state and dynamic performance of the proposed method is investigated using laboratory experiments with a 2.2-kW induction motor drive. The method improves the accuracy of the loss minimization and torque production, it does not require excessive computational resources, and it shows fast convergence to the optimum flux level

Publication VIII

The induction machine model parameters need to be estimated with good accuracy to ensure a good performance of the drive. Due to the magnetic saturation, the inductances vary as a function of the flux level. The magnetizing curve can be identified at standstill, but more accurate results are obtained if the identification is performed as the machine is running. In this paper, the magnetic saturation is modelled using a power function, and adaptation laws for the function parameters are proposed. The adaptation method is implemented in the control system of a sensorless drive. Experimental results on a 2.2-kW machine show that the identification of the stator inductance is rapid and the accuracy is good.

5.2 Contribution of the Thesis

The main contributions of the thesis can be summarized as follows:

- A small-signal model including the saturation of the magnetizing inductance and the rotor leakage inductance and the mutual saturation between these two is proposed. (Publication V)

- The influence of magnetic saturation on small-signal characteristics is analyzed. A comparison between the results of finite element analysis and experimental results is performed. (Publication I)

- An identification method for the leakage inductance taking the influence of the saturation on the transient characteristics into account is proposed. (Publication II)

- A model including the skin effect and the eddy currents in the rotor core as well as the magnetic saturation is proposed. The model is used in the identification of the leakage inductance. (Publication IV)

- A stator inductance identification method, where the parameters of the magnetizing curve are directly obtained is proposed. (Publication VIII)

- An iron loss model for the stator core losses of induction machines including both hysteresis and eddy current losses is proposed. (Publication III)

- The iron loss model is analyzed and experimentally validated for the case of a nonlinear inductor. (Publication VI)

- A loss-minimizing control algorithm of the induction machines based on the iron loss model is presented. (Publication VII)

6. Conclusions

Dynamic induction machine models are used as the basis for the design and implementation of control algorithms. The parameters of the model can be identified during the self-commissioning of the drive and as the machine is running. In order to ensure a good performance, the model should include the most relevant phenomena of the machine, and the parameters should be identified with a good accuracy.

In this thesis, the modeling of magnetic saturation and iron losses have been studied. Due to magnetic saturation, the inductances vary as the flux magnitude varies. The modeling of magnetic saturation is particularly demanding in machines having skewed or closed rotor slots, as the magnetic saturation cannot be modeled as dependent on a certain flux magnitude, such as the stator flux or main flux, but also the loading condition affects the inductances. A small-signal model including the saturation of the magnetizing inductance, the rotor leakage inductance and the mutual saturation between these two was proposed. The transient behavior of the induction machine was analyzed using the small-signal model. The magnetic saturation makes the machine appear to be salient in transients. The location of the saliency depends on the operating point. In a no-load condition, the location is determined by the direction of the magnetizing current vector, but as the load increases, the direction of the rotor current vector also affects the location of the saliency.

In order to include the influence of the load, the inductances of the machine should be identified during the operation of the machine. Especially the leakage inductance is affected by the load. A signal injection method for identifying the leakage inductance of the inverse-Γ model was proposed. The value obtained depends on the direction of the injected signal due to the saturation-induced saliency. The leakage inductance was measured in two directions, and by applying a coordinate transformation, the leakage inductance can be analyzed as a function of the angle of the reference frame. The resulting leakage inductance depends sinusoidally on the angle, and it was observed that the maximum value is closest to the operating-point value of the leakage inductance.

The stator inductance can be modeled by a rather simple function dependent on the stator flux magnitude. The parameters of the function were identified in an adaptive manner. Two different flux levels are necessary in order to obtain the entire saturation curve. The inductance is first identified in a non-saturated condition and then at a flux level close to the rated flux. In a no-load condition, the stator inductance can be obtained with good accuracy. A true no-load condition cannot, however, always be achieved, and the stator inductance estimate becomes sensitive to errors in the leakage inductance estimate. Particularly at low flux values, the sensitivity is high, and the leakage inductance needs to be estimated prior to the stator inductance.

The iron losses were modeled by a nonlinear resistance. The resistance can be seen as a parallel coupling of two resistances, one representing the eddy current losses and one representing the hysteresis losses. The eddy current loss resistance is constant, while the hysteresis loss resistance is dependent on the voltage and flux magnitude. As the frequency is not used in the iron loss model, the model can be used also during transients.

Topics for future research could include the differences of the stator inductance identification in generator and motor mode. The results are affected by the iron loss model, but also other phenomena could cause the differences. A more rapid identification method of the iron loss model could be developed. The implementation of the iron loss model would be easier if the iron loss resistance could be identified without time-consuming measurements at various flux levels and frequencies.

Bibliography

Aime, M. L., Degner, M. W. and Lorenz, R. D. (1998), Saturation measurements in AC machines using carrier signal injection, *in* 'Conf. Rec. IEEE-IAS Annu. Meeting', Vol. 1, St. Louis, MO, pp. 159–166.

Alger, P. L. (1965), *The Nature of Induction Machines*, Gordon and Breach, New York.

Bertoluzzo, M., Buja, G. S. and Menis, R. (2001), 'Self-commissioning of RFO IM drives: one-test identification of the magnetization characteristic of the motor', *IEEE Trans. Ind. Appl.* **37**(6), 1801–1806.

Blaschke, F., van der Burgt, J. and Vandenput, A. (1996), Sensorless direct field orientation at zero flux frequency, *in* 'Conf. Rec. IEEE-IAS Annu. Meeting', Vol. 1, San Diego, CA, pp. 189–196.

Boldea, I. and Nasar, S. A. (1987), 'Unified treatment of core losses and saturation in the orthogonal-axis model of electric machines', *Proc. IEE* **134**(6), 355–363.

Boldea, I. and Nasar, S. A. (1988), 'A general equivalent circuit (gec) of electric machines including crosscoupling saturation and frequency effects', *IEEE Trans. Energy Convers.* **3**(3), 689–695.

Bünte, A. and Grotstollen, H. (1993), Parameter identification of an inverter-fed indcution motor at standstill with a correlation method, *in* 'Proc. EPE'93', Vol. 5, Brighton, U.K., pp. 97–102.

Chua, L. O. and Stromsmoe, K. A. (1970), 'Lumped-circuit models for nonlinear inductors exhibiting hysteresis loops', *IEEE Trans. Circuit Theory* **CT-17**(4), 564–574.

Coussens, P. J., den Bossche, A. V. and Melkebeek, J. A. (1994), Parameter estimation for induction motor field oriented control using a non-linear motor model, *in* 'Proc. IEE PEVD Conf.', London, U.K., pp. 198–203.

de Jong, H. C. J. (1980), Saturation in electrical machines, *in* 'Proc. ICEM'80', Vol. 3, Athens, Greece, pp. 1545–1552.

Gastli, A. (1999), 'Identification of induction motor equivalent circuit parameters using the single-phase test', *IEEE Trans. Energy Convers.* **14**(1), 51–56.

Gerada, C., Bradley, K., Sumner, M. and Sewell, P. (2007), 'Evaluation and modeling of cross saturation due to leakage flux in vector-controlled induction machines', *IEEE Trans. Ind. Appl.* **43**(3), 694–702.

Healey, R. C., Williamson, S. and Smith, A. C. (1995), 'Improved cage rotor models for vector controlled induction motors', *IEEE Trans. Ind. Appl.* **31**(4), 812–822.

Hinkkanen, M., Repo, A.-K., Cederholm, M. and Luomi, J. (2007), Small-signal modelling of saturated induction machines with closed or skewed rotor slots, *in* 'Conf. Rec. IEEE-IAS Annu. Meeting', New Orleans, LA, pp. 1200–1206.

Holliday, D., Green, T. C. and Williams, B. W. (1994), On-line measurement of induction machine stator and rotor winding parameters, *in* 'Proc. IEE PEVD Conf.', London, U.K., pp. 485–469.

Jansen, P. L. and Lorenz, R. D. (1996), 'Transducerless field orientation concepts employing saturation-induced saliences in induction machines', *IEEE Trans. Ind. Appl.* **32**(6), 1380–1393.

Kerkman, R. J. (1985), 'Steady-state and transient analyses of an induction machine with saturation of the magnetizing branch', *IEEE Trans. Ind. Appl.* **IA-21**(1), 226–234.

Kerkman, R. J., Thunes, J. D., Rowan, T. M. and Schlegel, D. W. (1996), 'A frequency-based determination of transient inductance and rotor resistance for field commissioning purposes', *IEEE Trans. Ind. Appl.* **32**(3), 577–584.

Klaes, N. R. (1993), 'Parameter identification of an induction machine with regard to dependencies on saturation', *IEEE Trans. Ind. Appl.* **IA-29**(6), 1135–1140.

Kwon, Y.-S., Lee, J.-H., Moon, S.-H., Kwon, B.-K., Choi, C.-H. and Seok, J.-K. (2009), 'Standstill parameters identification of vector-controlled induction motors using the frequency characteristics of rotor bars', *IEEE Trans. Ind. Appl.* **45**(5), 1610–1618.

Laldin, O., Dlala, E. and Arkkio, A. (2011), 'Circuit models for predicting core losses in the stator and rotor of a caged induction machine with sinusoidal supplies', *IEEE Trans. Magn.* **47**(5), 1054–1057.

Levi, E. (1997), 'General method of magnetising flux saturation modelling in d-q axis models of double-cage induction machines', **144**(2), 101–109.

Levi, E., Sokola, M., Boglietti, A. and Pastorelli, M. (1996), 'Iron loss in rotor-flux-oriented induction machines: identification, assessment of detuning and compensation', *IEEE Trans. Power Electronics* **11**(5), 698–709.

Levi, E. and Vukosavic, S. N. (1999), 'Identification of the magnetising curve during commissioning of a rotor flux oriented induction machine', *IEE Proc. Electr. Power Appl.* **146**(6), 685–693.

Lin, C. E., Wei, J.-G., Huang, C.-L. and Huang, C.-J. (1989), 'A new model for transformer saturations characteristics by including hysteresis loops', *IEEE Trans. Magn.* **25**(3), 2706–2712.

Melkebeek, J. A. A. and Novotny, D. (1983), 'The influence of saturation on induction machine drive dynamics', *IEEE Trans. Ind. Appl.* **19**(5), 671–681.

Menemenlis, N. (1998), 'Noniterative dynamic hysteresis modelling for real-time implementation', *IEEE Trans. Power Systems* **13**(4), 1556–1563.

Monjo, L., Córcoles, F. and Pedra, J. (2013), 'Saturation effects on torque- and current-slip curves of squirrel-cage induction motors', *IEEE Trans. Energy Convers.* **28**(1), 243–254.

Moon, S.-I., Keyhani, A. and Pillutla, S. (1999), 'Nonlinear neural-network modeling of an induction machine', *IEEE Trans. Control Syst. Technol.* **7**(2), 203–211.

Nerg, J., Pyrhönen, J., Partanen, J. and Ritchie, E. (2004), Induction motor magnetizing inductance modelling as a function of torque, *in* 'Proc. ICEM'04', Cracow, Poland. CD-ROM.

Neves, W. and Dommel, H. (1993), 'On modelling iron core nonlinearities', *IEEE Trans. Power Systems* **8**(2), 417–425.

Ojo, J. O., Consoli, A. and Lipo, T. A. (1990), 'An improved model of saturated induction machines', *IEEE Trans. Ind. Appl.* **26**(2), 212–221.

Proca, A. B. and Keyhani, A. (2002), 'Identification of variable frequency induction motor models from operating data', *IEEE Trans. Energy Convers.* **17**(1), 24–31.

Qu, Z., Ranta, M., Hinkkanen, M. and Luomi, J. (2011), Loss-minimizing flux level control of induction motor drives, *in* 'Proc. IEEE IEMDC'11', Niagara falls, Canada.

Ranta, M. and Hinkkanen, M. (2012), Online identification of parameters defining the saturation characteristics of induction machines, *in* 'Proc. ICEM'12', Marseille, France.

Rasmussen, H., Knudsen, M. and Tønnes, M. (1996), Parameter estimation of inverter and motor model at standstill using measured currents only, *in* 'Proc. IEEE ISIE'96', Vol. 1, Warsaw, Poland, pp. 331–336.

Retière, N. M. and Ivanès, M. S. (1999), 'An introduction to electric machine modeling by systems of non-integer order. Application to double-cage induction machine', *IEEE Trans. Energy Convers.* **14**(4), 1026–1032.

Schierling, H. (1988), Self-commissioning - a novel feature of modern inverter-fed induction motor drives, *in* 'Proc. IEE PEVD Conf.', Vol. 1, London, U.K., pp. 287–290.

Shinnaka, S. (2001), 'Proposition of new mathematical models with stator core loss factor for induction motor', *Electr. Eng. in Japan* **134**(1), 64–75.

Slemon, G. R. (1989), 'Modelling of induction machines for electric drives', *IEEE Trans. Ind. Appl.* **25**(6), 1126–1131.

Sudhoff, S. D., Aliprantis, D. C., Kuhn, B. T. and Chapman, P. L. (2002), 'An induction machine model for predicting inverter-machine interaction', *IEEE Trans. Energy Convers.* **17**(2), 203–210.

Sukhapap, C. and Sangwongwanich, S. (2002), Auto tuning of parameters and magnetization curve of an induction motor at standstill, *in* 'Proc. IEEE ICIT'02', Vol. 1, Bangkok, Thailand, pp. 101–106.

Sullivan, C. R. and Sanders, S. R. (1995), 'Models for induction machines with magnetic saturation of the main flux path', *IEEE Trans. Ind. Appl.* **31**(4), 907–917.

Sumner, M. and Asher, G. M. (1993), 'Autocommissioning for voltage-referenced voltage-fed vector-controlled induction motor drives', *IEE Proc. B, Electr. Power Appl.* **140**(3), 187–200.

Tuovinen, T., Hinkkanen, M. and Luomi, J. (2010), 'Modeling of saturation due to main and leakage flux interaction in induction machines', *IEEE Trans. Ind. Appl.* **46**(3), 937–945.

White, T. J. and Hinton, J. C. (1995), Compensation for the skin effect in vector-controlled induction motor drive systems, *in* 'Conf. Proc. IEE Elect. Mach. Drives', pp. 301–305.

Williamson, S. and Begg, M. C. (1985), 'Calculation of the bar resistance and leakage reactance of cage rotors with closed slots', *IEE Proc. B, Electr. Power Appl.* **132**(3), 125–132.

Williamson, S. and Healey, R. C. (1996), 'Space vector representation of advanced motor models for vector controlled induction motors', **143**(1), 69–77.

Wlas, M., Krzemiński, Z. and Toliyat, H. A. (2008), 'Neural-network-based parameter estimations of induction motors', *IEEE Trans. Ind. Electron.* **55**(4), 1783–1794.

Yahiaoui, A. and Bouillault, F. (1995), 'Saturation effect on the electromagnetic behaviour of an induction machine', *IEEE Trans. Magn.* **31**(3), 2036–2039.

Zamora, J. L. and García-Cerrada, A. (2000), 'Online estimation of the stator parameters in an induction motor using only voltage and current measurements', *IEEE Trans. Ind. Appl.* **36**(3), 805–816.

The induction machine is the most common electrical machine. The speed of the machine can be controlled by connecting a frequency converter to the machine. By applying speed-sensorless techniques, the cost of the drive can be reduced and the reliability can be improved. The operation of a speed-sensorless drive requires a good model of the induction machine. Furthermore, the identification of model parameters might require modelling of transient phenomena. In this thesis, the modelling of magnetic saturation and iron losses of an induction machine is studied. The transient behavior of the machine is analysed using a small-signal model, and identification methods for the inductances are developed. The iron losses are modelled by a nonlinear resistance, and the models are experimentally verified.

Aalto-DD 171/2013

9789526053950

ISBN 978-952-60-5395-0
ISBN 978-952-60-5396-7 (pdf)
ISSN-L 1799-4934
ISSN 1799-4934
ISSN 1799-4942 (pdf)

Aalto University
School of Electrical Engineering
Department of Electrical Engineering
www.aalto.fi

BUSINESS +
ECONOMY

ART +
DESIGN +
ARCHITECTURE

SCIENCE +
TECHNOLOGY

CROSSOVER

**DOCTORAL
DISSERTATIONS**